Spatiotemporal dynamics of HF-induced ionospheric turbulence revealed by diagnostic stimulated electromagnetic emission and test radio waves at HAARP

E E. N. Sergeev[1], S. M. Grach[1], A. V. Shindin[1], E. V. Mishin[2], P. A. Bernhardt[2], S. J. Briczinski[3], M. McCarric[3]

[1]*Lobachevsky State University, Nizhny Novgorod Russia*
e-mail: esergeev@nirfi.unn.ru
[2]*Space Vehicles Directorate, Air Force Research Laboratory, Kirtland AFB, USA*
[3]*Plasma Physics Division, Naval Research Laboratory, Washington, USA*

Abstract

We report on the dynamics of the HF-pumped ionosphere explored using measurements of stimulated electromagnetic emissions (SEE) and anomalous absorption of test radiowaves during the March 2011 HAARP heating experiments. In addition to the SEE excited by quasi-continuous pump waves (QCP), short-pulse test or diagnostic waves at frequencies shifted from the pump frequency excited diagnostic SEE (DSEE). Such an experimental setup allowed studying the dynamic spectra and damping rates of the plasma waves related to both test and QCP waves, as well as the QCP-related small-scale magnetic field-aligned irregularities (striations) inside the heated volume.

Introduction

It is well known that Langmuir modes are excited near the PW reflection point, $f_{pe}(h_r)= f_0$, in a few milliseconds after the arrival of a high-power HF radiowave (hereafter, the pump wave, PW). Here f_{pe} is the plasma frequency and f_0 is the PW frequency. Langmuir waves cause the so-called ponderomotive narrow continuum feature (NCp) of stimulated (or secondary) electromagnetic emissions (SEE) red-shifted by up to 40 kHz from f_0, i.e., $|\Delta f_{NC}|= f_0 - f_{NC} <40$ kHz. The long-term, >0.5 s, HF pumping leads to excitation of the Z-mode and/or upper-hybrid (UH) quasi-electrostatic waves, as well as short-scale, 0.5-50 m across the magnetic field, field-aligned irregularities (striations). The strongest interaction between the pump, UH waves, and striations occurs near the UH height $h_0 < h_r$, where the UH frequency $f_{UH} = (f_{pe}^2 + f_{ce}^2)^{1/2}$ matches f_0 (f_{ce} is the electron cyclotron frequency). Transfer of the UH wave energy over frequencies and their scattering on striations leads to generation of the UH-related SEE features, such as the Downshifted Maximum (DM), $f_{DM} \approx f_0 - 10$ kHz, Broad Continuum (BC), -60 kHz< $\Delta f_{BC}=f_{BC} - f_0 <0$ and Upshifted Maximum (UM) at $\Delta f_{UM}=f_{UM} - f_0 \approx - \Delta f_{DM}$ [1,2].

A typical dimension of the excited striations along the geomagnetic field, $l_{\|}$, is of the order of 5-30 km. It is close to the altitudinal extent of the heated region and the F-region thickness at the Sura, HAARP, and EISCAT facilities with χ = 18.5°, 14.5°, and 12°, respectively (χ is the conjugate to the magnetic dip angle). The altitudes of the upper-hybrid resonances (h_D) for the diagnostic waves at frequencies f_D and the pump wave (h_0) at the frequency f_0 ($f_D \neq f_0$) can significantly differ from each other. Therefore, measuring the diagnostic SEE (DSEE) generated by a short-pulse diagnostic wave (DW) will specify the DW-related Z/UH modes as well as the QCP related striations near h_D. Applying different frequencies f_D will provide the relevant information at different altitudes in the perturbed region. Additional information on the striation intensity can be revealed from measurements of anomalous absorption (AA) of the sounding (S) waves. AA is consequent to conversion of electromagnetic waves including QCP, D, S, SEE, and DSEE on striations into Z/UH waves. As a result, the QCP and DW are shielded from the reflection point so the NCp generation is inhibited.

Investigation of the HF-pumped ionosphere using DSEE and diagnostic waves had been performed earlier at the SURA heating facility [3-5]. This paper presents the results of similar experiments at the HAARP heating facility on March 28, 2011 at 16:45 -17:45 AST.

Experimental setup

Each 5 min transmitting cycle comprises several duty cycles as follows. For initial 30 s, the primary pump wave with the effective radiated power (ERP) P_{ef} =400 MW is transmitted vertically at f_0 = 5450 kHz in the low-duty diagnostic (D) regime (f_0^D=f_0), with the pulse width τ_D=20 ms and the interpulse period T_D=1 s. Next 60 s, the pumping continues in the high-duty quasi-continuous regime, QCP, with τ_Q=160 ms and T_Q=200 ms. Then, the pumping is switched back to the D-regime for 210 s. During the whole 5 min period, the secondary pump wave at f_D=f_0 + δf is radiated in the D regime, with the frequency offset δf = -200 kHz and the same ERP of 400 MW. In addition, very short, τ_S=100 μs, sounding (S) pulses lagging the pump waves by 180 ms are injected at the same ERP and carrier frequencies, f_S =f_0 and f_S^D= f_D, with the interpulse period T_S=200 ms. Both primarily and secondary pump and S waves are of the ordinary polarization. The next 5 min cycle starts after a 1 min intermission, with the primary and secondary pump frequencies being interchanged, i.e., f_D= 5450 kHz, f_0=f_D + δf. Then, after the 1 min intermission, the whole 12 min sequence is repeated with $|\delta f|$ increased by 200 kHz.

Due to the time lag of 180 ms, the S-pulses are placed in the 40 ms pauses of the QCP regime. They create a broad spectrum of diagnostic waves (up to 300 kHz near each carrier frequency). The QCP and D regimes are used to create plasma turbulence, particularly striations, and to generate DSEE at different altitudes both with and without QCP, respectively. The SEE and DSEE measurements during first 20 ms of the QCP 40 ms pause and just after diagnostic 20 ms pulses allow measuring the SEE relaxation time, and thus the damping time of the plasma waves that generate SEE and DSEE. The S-pulses reveal anomalous absorption of the QCP, D and S waves *vs*. frequency due to conversion on striations into upper hybrid waves.

The ambient ionosphere conditions in the course of the experiment were stable so that the reflection altitude of the pump wave at 5450 kHz varied in the range 205-210 km. Overall, the frequency offsets δf = ±200, ±400, ±600, ±800 and ±1000 kHz were used. The corresponding reflection altitudes of the primary and secondary pump waves differed by 5-6 km, 8-9 km, 13-17 km, 18-21 km, and 24-25 km, respectively.

Experimental results

Figure 1 displays the SEE and DSEE spectrograms generated during the QCP and D regimes for the third and fourth cycles with $|\delta f|$=400 kHz that correspond to frames [05]-[08] in Figs. 2 and 3. The first and second frames on the left show the DSEE and SEE spectrograms for f_0 = 5450 kHz and the DSEE spectrogram for f_D = 5050 kHz, respectively. The next two frames show those for f_0 = 5050 and f_D = 5450 kHz. The black bars indicate the QCP regime. The DSEE spectra are obtained in the time window from 10 to 20 ms of each diagnostic pulse, the SEE spectra during QCP (for t=0-60 s in frames 1 and 3) are recorded simultaneous with the DSEE spectra.

Figure 2 presents the DSEE spectra before the QCP regime is turned on (averaged over the time intervals t = –30 - 0 s, gray lines) and during the QCP regime (averaged over t=40-60 s, columns 2 and 4, black lines), as well as the steady state SEE spectra averaged over t=30-60 s (columns 1 and 3, black lines) for the whole experiment. Figure 3 shows the SEE and DSEE temporal dynamics at the frequency shifts corresponding to the UH-related features, such as the DM (Δf_{DM} = –10 kHz, black) and the BC (Δf_{BC}= – 20 kHz in frames [01] and [04], and Δf_{BC}= – 40 kHz in the other frames, gray).

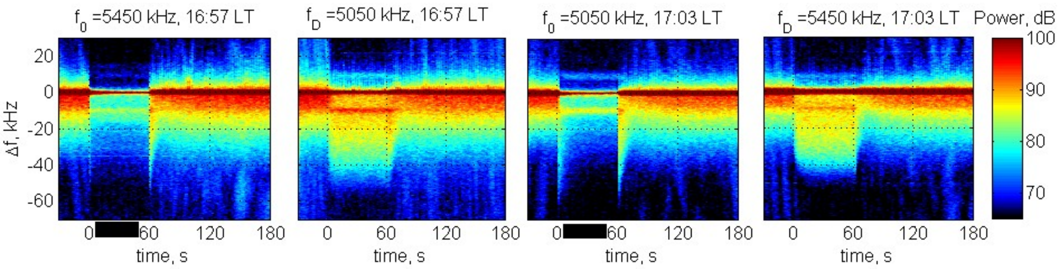

Figure 1. SEE and DSEE spectrograms during the QCP and D regimes with $|\delta f|$ = 400 kHz corresponding to frames [05]-[08] in Figs. 2 and 3. From left to right: DSEE/SEE spectrogram for QCP with f_0=5450 kHz; DSEE spectrogram for f_D=5050 kHz and f_0=5450 kHz, DSEE/SEE spectrogram for QCP with f_0=5050 kHz; DSEE spectrogram for f_D=5450 kHz and f_0=5050 kHz The black bars indicate the QCP regime (0-60 s) in the panels with SEE spectrograms..

The time of the QCP radiation (0-60 s) are shown by black bars under the panels with SEE spectrograms.

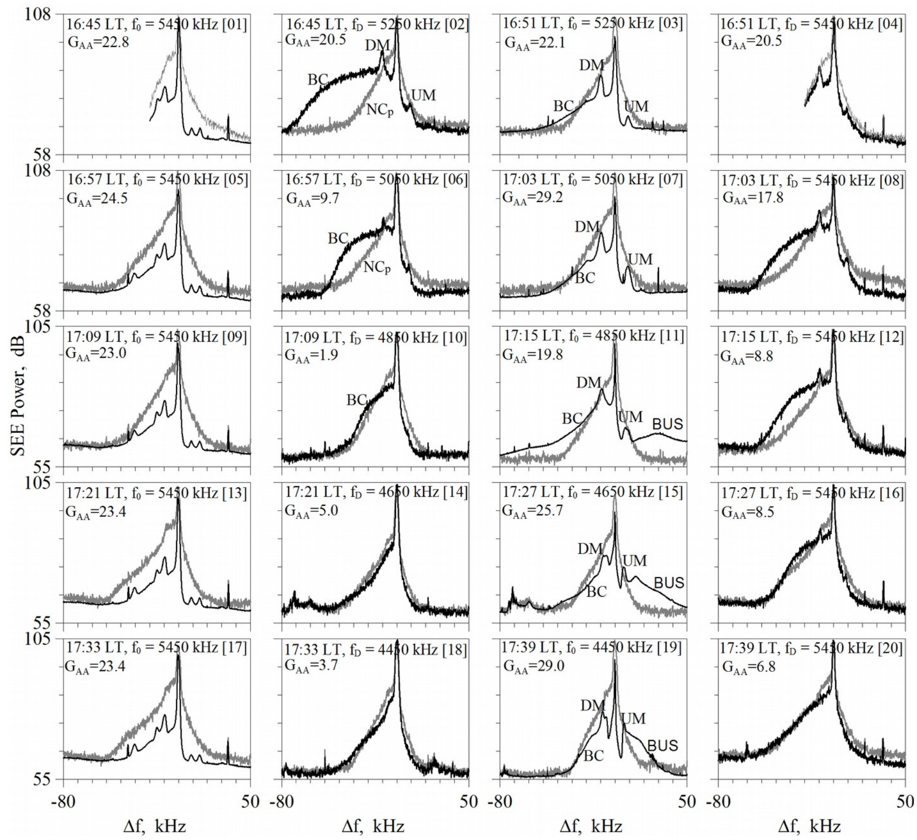

Figure 2. (left column) SEE spectra for f_0=5450 kHz during QCP (30-60 s, black), (2nd column) DSEE for different D-wave frequencies f_D during QCP (40-60 s, black) at f_0=5450 kHz, (3rd) SEE for different f_0 (black), (right) DSEE related to f_D= 5450 kHz during QCP (black) at different f_0. The gray lines indicate DSEE during the D-regime before QCP, i.e., from – 30 to 0 s. The SEE/DSEE spectral features, such as the NCp, DM, BC, UM, and BUS are indicated. The time and number of each cycle, with the pump frequencies f_0 and f_D and the magnitude of the S-wave anomalous absorption at f_S=$f_{0,D}$ in dB (G_{AA}), are shown.

During the diagnostic regime before the QCP regime is turned on and approximately 20 s after the QCP is turned off, the DSEE spectra show only Langmuir-related NCp feature generated near the reflection points of the primary and secondary pump waves. After the QCP turn-on, the NCp suffers strong suppression due to anomalous absorption. On the contrary, for f_0=f_D the DM and BC are intensified and exhibit the overshoot effect, i.e., the intensity drops after achieving the maximum. Even stronger overshoots of the DM and BC appear when QCP is switched to the D-regime. Notice also, that both first and second overshoots are relatively stronger for larger $|\Delta f|$.

These overshoots after QCP is turned on (off) are readily explained in terms of the competition between the increase (decrease) of the AA and growth (fall) of the SEE source due to developing (relaxing) striations [1, 5, 6]. The obtained *e*-folding time of the DSEE intensity relaxation from pulse to pulse after the reaching the maximum was 2-5 s. The maximum overshoot, i.e., the ratio of the SEE intensity at the maximum to that at the steady state of 10-15 dB occurs at the primary pump frequency f_0 in the center of the pumped volume near h_0. The SEE spectra at f_0=4850 kHz, 4650 kHz and 4450 kHz (panels 11, 15 19) contain also broad upshifted structure (BUS) at Δf_{BUS} ~ 10-50 kHz, the typical SEE feature for $150 \leq f_0 - sf_{ce} \leq 400$ kHz (here s=3 is the gyroharmonic number) [2].

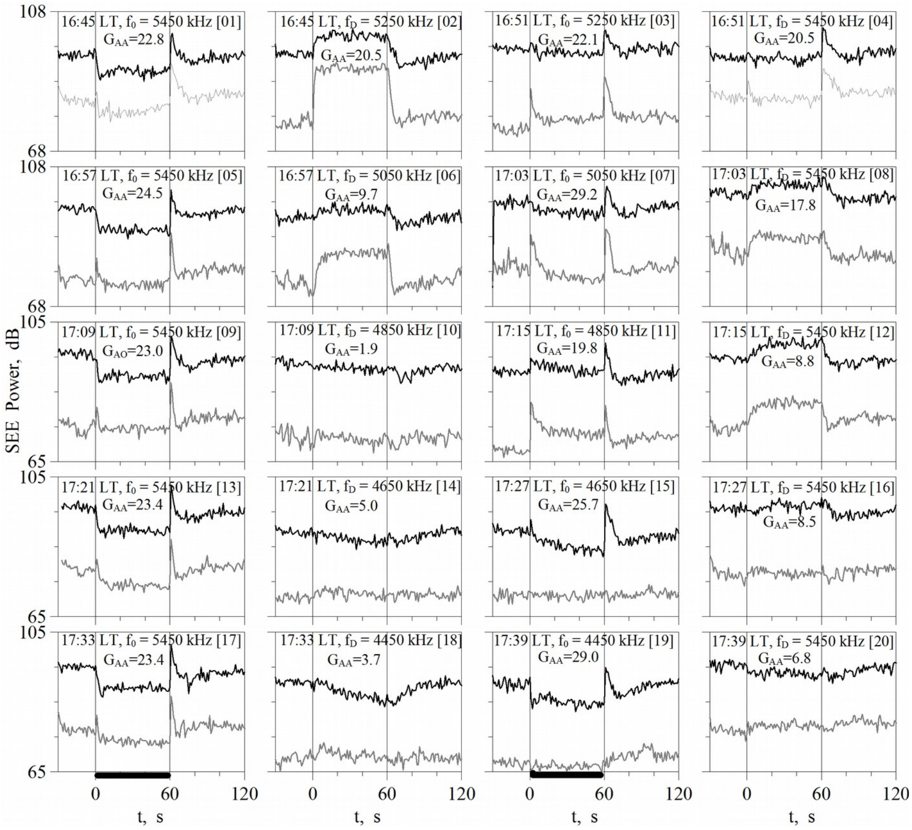

Figure 3. Dynamics of the SEE and DSEE at frequency shifts corresponding to the UH-related features DM (Δf_{DM} = –10 kHz, black) and BC (Δf_{BC}= – 20 kHz for the panels [01] and [04], and Δf_{BC}= – 40 kHz for other panels, gray). The distribution of panels over experimental sessions is the same as in Figure 2.

The DM, BC and UM features in the SEE spectra are generated for all QCP frequencies used (Fig 2 columns 1,3,), while for DSEE with $f_D \neq f_0$ these features during QCP are well distinguished for δf=200, 400, 600, 800 kHz, i.e. $h_D - h_0 \leq 20$ km, and for δf= –200 and –400 kHz, i.e. $h_0 - h_D \leq$ 9 km. The QCP-on/off overshoots for DSEE with $f_D \neq f_0$ are much weaker, if exist at all. They are notable only during sounding of the upper part of the heated volume, $h_D - h_0 < 10$ km, i.e., for δf = 200, 400 kHz. Instead, the monotonous growth of the DM and BC features of the DSEE after the QCP switch on is observed for the offsets δf= –200, –400 kHz, i.e., in the lower part of the heated volume at $h_0 - h_D < 10$ km, and δf= 600, 800 kHz i.e., in the upper part at $10 < h_D - h_0 < 20$ km. At δf= –600, –800 kHz, $10 < h_0 - h_D < 20$ km, as well as for δf = 1000 kHz, $h_D - h_0$ ~ 25 km the competition between Langmuir-related (NCp) and UH-related (DM and BC) DSEE features was obtained during QCP. For δf = – 1000 kHz, $h_0 - h_D$~25 km, a slow suppression of the NC is obtained due to AA development, and the DM is not seen in the DSEE spectrum.

Figure 4 illustrates the NCp decay after 20-ms pulses (frames *a* and *c*) and that of the UH-related SEE and DSEE features during 40-ms pauses (*b* and *c*) at different frequency shifts $\Delta f = f_{SEE} - f_{0,D}$. Figure corresponds to sessions shown in Figure 1 and second row in Figures 2 and 3. It is established that 1) during QCP the decay time of the UH-related SEE features (in the center of heated volume, panel *b*) is shorter than that of the UH-related DSEE features in the heated volume periphery (panel *c*); 2) the decay time of the Langmuir related NCp (τ_d ~3.1-3.3 ms) is longer than that of the UH related SEE and DSEE features and close to the collisional plasma wave damping rate.

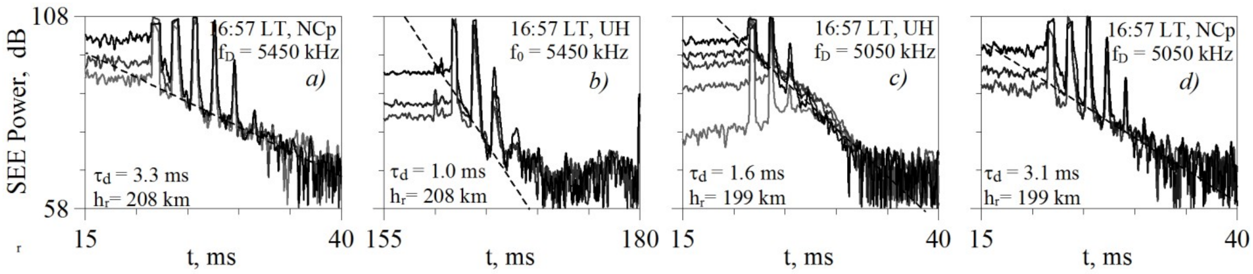

Figure 4. Variation of the DSEE after 20-ms pulses and SEE during 30 ms pauses in QCP at different frequency shifts corresponding to frame [05] in Figs. 2 and 3. (*a*) and (*d*): the NCp feature without QCP; (*b*) the SEE and (*c)* DSEE features related to UH waves. . The primary pump wave (QCP) frequency f_0=5450 kHz. The SEE/DSEE decay time τ_d and reflection heights of the D and QCP waves h_r are shown in the frames. The step between the frequency offsets for different lines is 5 kHz for the NCp and 10 kHz for the UH-related SEE features starting from Δf = –11 kHz (the upper line).

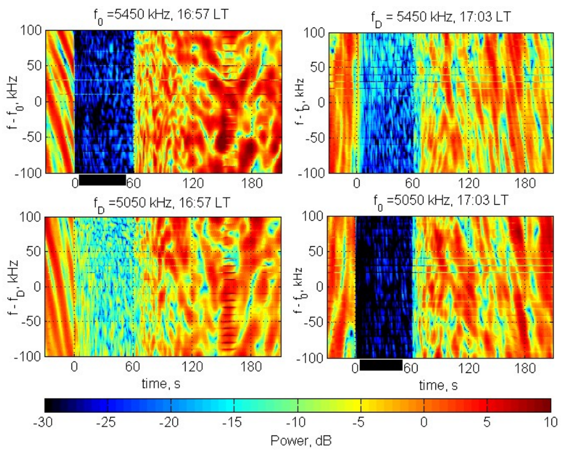

Figure 5. Spectrograms of the reflected sounding waves for (top left) f_S=f_0 =5450 kHz and (bottom, left) f_S=f_D=5050 kHz, (bottom, right) f_S=f_0=5050 kHz and (top, right) f_S=f_D=5450 kHz, corresponding to the frames [05], [06], [07] and [08] in Figs 2,3, respectively. The black bar indicates the QCP regime.

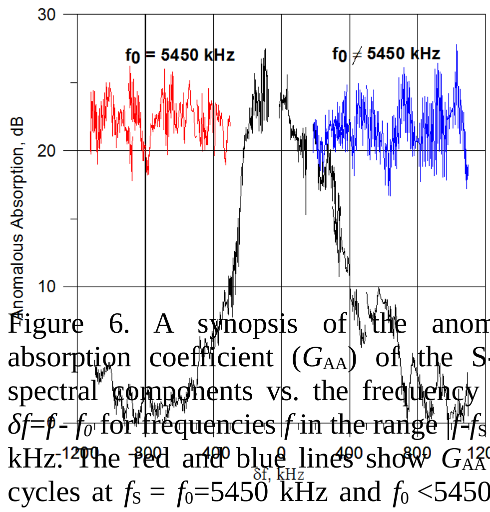

Figure 6. A synopsis of the anomalous absorption coefficient (G_{AA}) of the S-wave spectral components vs. the frequency offset δf=f - f_0 for frequencies f in the range $|f$-$f_S|$<100 kHz. The red and blue lines show G_{AA} for 5 cycles at f_S = f_0=5450 kHz and f_0 <5450 kHz, respectively. The black line shows G_{AA} for f > f_0 (on the right) at f_0 < f_S = f_D =5450 kHz and for f< f_0 (on the left) at f_D< f_0=5450 kHz.

Figure 5 presents spectrograms of the reflected sounding waves that illustrate anomalous absorption during the cycles in Fig. 1. The anomalous absorption coefficient is G_{AA} = 10 log10 (S_1/S_2), where S_1 and S_2 are intensities of the reflected sounding wave spectral components during D and QCP regimes, respectively. The frequency dependence of G_{AA} is shown in Fig. 6. Note that the values of G_{AA} at f = f_0 are reduced from the observed values to the mean value for f_0=5450 kHz, while the value of G_{AA} at f = f_D are shifted by the latter reduction. The observed AA magnitudes for f_S=f_0 and f_S=f_D are shown in Fig. 3. It is seen that the AA magnitude maximizes (G_{AA} ~25 dB) at the center of the heated volume for f_S~f_0 and decreases down to 2-3 dB with $|f$ - $f_0|$, i.e., towards the periphery. Interestingly, G_{AA} decreases faster at negative offsets or h_0>h_D.

Discussion

The spatiotemporal dynamics of the artificial ionospheric turbulence is explored by means of SEE generated by short-pulse diagnostic waves at frequencies f_D shifted from the QCP pump wave frequency f_0 and measurements of anomalous absorption at HAARP. The basic features include the presence or absence of the UH-related DSEE overshoots depending on the distance of the source from the center of the heated volume, the increase of the DSEE decay time and decrease of anomalous absorption towards the periphery of the heated volume. These features can be understood in terms of three interrelated steps: (a) excitation of striations and UH waves near the UH resonance of the primary pump wave and scattering (at the developed stage) of the primary and secondary pump waves into UH waves on striations near the corresponding UH resonances, (b) formation of the red- and blue-shifted sidebands around $f_{0,D}$ in the UH spectrum, and (c) conversion of UH waves into electromagnetic waves on striations. One of the key factors that determine the resulting parameters is the dependence of the intensity and spatial spectrum of striations excited by the primary pump wave on altitude [6]. The similarity of these results with that obtained earlier at the "Sura" facility with much smaller ERP remain to be understood, as well as the asymmetry of the DSEE and AA behavior relative to the center of the heated volume.

References

1. Grach S. M., Sergeev E. N., Mishin E. V., Shindin A. V., Dynamic properties of ionospheric plasma turbulence driven by high-power high-frequency radiowaves, Physics – Uspekhi, 2016, 59 (11) 1091 - 1128, DOI: https://doi.org/10.3367/UFNe.2016.07.037868
2. Leyser T.B. , Stimulated electromagnetic emissions by high-frequency electromagnetic pumping of the ionospheric plasma, Space Sci. Rev., 2001, 98 (3-4). 223 -328
3. Frolov V. L., Boiko G. N., Metelev S. A., Sergeev E. N., On the study of artificial ionospheric turbulence by means of stimulated electromagnetic emission, Radiophys. and Quantum Electron., 1994, 37 (7), 593-603.
4. Sergeev E. N., Frolov V. L., Boiko G. N., Results of investigation of the langmuir and upper-hybrid plasma turbulence evolution by means of stimulated ionospheric emission, Radiophys. and Quantum Electron., 1998, 41 (3), 206-228.
5. Sergeev E. N., Grach S. M., Komrakov G. P. et al., Influence of small-scale irregularities on the features of the overshoot effect in the temporal evolution of stimulated electromagnetic emission. Part I. Development stage, Radiophys. and Quantum Electron., 1999, 42 (7), 544-656, Part II. Relaxation stage, Radiophys. and Quantum Electron., 1999, 42 (8), 715-727.
6. Sergeev E.N., Grach S.M. Study of the plasma turbulence dynamics by measurements of diagnostic stimulated electromagnetic emission. I. Experimental results, Radiophys. Quantum Electron., 2014, 57 (2), 81-99, II. Results of numerical simulation, Radiophys. Quantum Electron., 2017, 60 (2)